Heliyon 10 (2024) e33736

Contents lists available at ScienceDirect

Heliyon

journal homepage: www.cell.com/heliyon

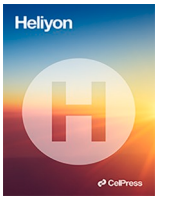

Research article

Reprogramming human urine cells into intestinal organoids with long-term expansion ability and barrier function

Ruifang Zhang [a,b,1], Yating Chen [a,b,1], Ziyu Feng [b], Baomei Cai [b], Yiyi Cheng [a], Yunjing Du [e], Sihua Ou [b], Huan Chen [b], Mengjie Pan [b], He Liu [d], Duanqing Pei [c,**], Shangtao Cao [a,b,*]

[a] *Key Laboratory of Biological Targeting Diagnosis, Therapy, and Rehabilitation of Guangdong Higher Education Institutes, The Fifth Affiliated Hospital of Guangzhou Medical University, Guangzhou, Guangdong, China*
[b] *Guangzhou Medical University, Guangzhou National Laboratory, Guangzhou, Guangdong, China*
[c] *Laboratory of Cell Fate Control, School of Life Sciences, Westlake University, Hangzhou, China*
[d] *Bioland Laboratory (Guangzhou Regenerative Medicine and Health Guangdong Laboratory), Guangzhou, Guangdong, China*
[e] *School of Biosciences & Biopharmaceutics, Guangdong Pharmaceutical University, Guangzhou, China*

ARTICLE INFO

Keywords:
Intestinal organoids
Human urine cells
Reprogramming
Metallothionein
CYP450

ABSTRACT

Generation of intestinal organoids from human somatic cells by reprogramming would enable intestinal regeneration, disease modeling, and drug screening in a personalized pattern. Here, we report a direct reprogramming protocol for the generation of human urine cells induced intestinal organoids (U-iIOs) under a defined medium. U-iIOs expressed multiple intestinal specific genes and showed resembling gene expression profiles to primary small intestines. U-iIOs can be stably long-term expanded and further differentiated into more mature intestinal lineage cells with high expression of metallothionein and cytochrome P450 (CYP450) genes. These specific molecular features of U-iIOs differ from human pluripotent stem cells derived intestinal organoids (P-iIOs) and intestinal immortalized cell lines. Furthermore, U-iIOs exhibit intestinal barriers indicated by blocking FITC-dextran permeation and uptaking of the specific substrate rhodamine 123. Our study provides a novel platform for patient-specific intestinal organoid generation, which may lead to precision treatment of intestinal diseases and facilitate drug discovery.

1. Introduction

The intestine is one of the most important organs responsible for digestive function and nutrient absorption in the human body. These functions rely on the intact and complex architecture of intestinal epithelia which possess numbers of transporters and enzymes [1]. Despite their recapitulation capacity of certain aspects of intestinal functions in 2D culture, adenocarcinoma cell lines like Caco-2 don't fully reflect cell phenotypes and communications *in vivo*. Recently, a substantial breakthrough in the 3D intestinal organoids culture made it accessible to satisfactorily reconstitute intestinal structure, organization, and functionality *in vitro* to investigate

* Corresponding author. Key Laboratory of Biological Targeting Diagnosis, Therapy, and Rehabilitation of Guangdong Higher Education Institutes, The Fifth Affiliated Hospital of Guangzhou Medical University, Guangzhou, Guangdong, China.
** Corresponding author.
E-mail addresses: peiduanqing@westlake.edu.cn (D. Pei), cao_shangtao@gzlab.ac.cn (S. Cao).
[1] These authors contributed equally: Ruifang Zhang, Yating Chen.

https://doi.org/10.1016/j.heliyon.2024.e33736
Received 21 December 2023; Received in revised form 25 June 2024; Accepted 26 June 2024
Available online 27 June 2024

intestinal epithelium's roles in development and disease [2,3]. Since LGR5 was uncovered to specifically label intestinal stem cells located in the crypt [4], intestinal organoids were generated from isolated LGR5+ stem cells and further optimized to expand long-term *in vitro* via the intervention of signaling pathways like WNT, TGF-β, and YAP as well as epigenetic regulation [5]. However, due to limited healthy intestinal tissues and invasive procedures, it is difficult to obtain enough tissues to produce large-scale human intestinal organoids for clinical applications. As an alternative, scientists worldwide have made efforts to develop methods for intestinal organoid induction from human embryonic stem cells (hESCs) or induced pluripotent stem cells (hiPSCs). Moreover, as hiPSCs are reprogrammed from somatic cells, hiPSCs-derived intestinal organoids (P-iIOs) provide a valuable *in vitro* model to study intestinal development and diseases in a personalized manner [6–8]. However, recent studies suggest that human pluripotent stem cells have the potential to develop into tumors as a result of incomplete differentiation [9–13], which may hamper their use for regenerative medicine purposes.

One potential approach to overcome such obstacles is to generate intestinal organoids by, direct reprogramming of differentiated somatic cells bypassing the pluripotent state [14]. Thus far, human fibroblasts have been efficiently converted into three germ-layer lineage cells including endodermal progenitor cells, neural cells [15], hepatocytes [16], and cardiomyocytes by defined factors or small molecules [17]. It is reported that different initiator cells tended to be reprogrammed into functional cells with certain features because of their specific genetic molecular state as well as epigenetic memory. Compared with fibroblasts, human urine cells (hUCs) have some advantages as initiator cells to be reprogrammed. Apart from convenient sample collection, isolation, and culture via noninvasive ways, hUCs are typical epithelial cells and contain abundant mitochondria and transporters, which implies that hUCs may be easier to reprogram into certain functional cells. We previously reported that hUCs were robustly reprogrammed into iPSCs and neural progenitor cells dispensing with going through mesenchymal to epithelial transition (MET) which was required for somatic cell reprogramming [18–20]. Recently, we also efficiently converted hUCs into mesodermal progenitor cells and then established mitochondria-rich kidney organoids and somitoids respectively without passing through a pluripotent state [21]. In addition, we directly reprogrammed hUCs into cardiomyocytes by defining factors excluding GATA4 which is essential for cardiac reprogramming from fibroblasts [22]. Collectively, our previous work suggested that hUCs were highly plastic for cell fate transition. Thus, considering intestinal epithelial cells are also rich in mitochondria and transporters for absorption and metabolism, we wondered whether hUCs could be reprogrammed into intestinal epithelial cells for intestinal organoid generation with special characteristics.

In this report, we established one direct reprogramming method for hUCs-induced intestinal organoids (U-iIOs) generation and expansion long-term *in vitro* under a defined medium. Our results revealed that U-iIOs have a high expression of metallothionein and cytochrome P450 (CYP450) genes, which is different from P-iIOs and immortalized intestinal cell lines. This new platform may allow us to further investigate intestinal stem cell biology as well as disease modeling and drug screening in a personalized fashion.

2. Materials and methods

2.1. Human urine cells isolation and culture

Mid-stream urine samples from healthy female and male volunteers (aged 20–35 years) were collected and then stored at 4 °C for 4 h before isolation. Typical specimen volumes were 50–200 mL. Human urine cells (hUCs) were harvested by centrifugating the urine at 500×*g* for 8 min. The collected cells were then washed with DPBS supplemented with 1 × penicillin/streptomycin (Hyclone, SH40003.01) twice and cultured in gelatin-coated 6-cm dishes. The basic urine cell culture medium (UCCM) we used was a one-to-one mixture of Renal Epithelial Growth Medium (REGM, LONZA, CC-3191) and DMEM High Glucose (Hyclone, SH30022.01) containing 10 % FBS, 1 × L-GlutaMAX (GIBCO, 35050-061), and 1 × non-essential amino acids (NEAA; GIBCO, 11140-050). The washed cells were cultured with the UCCM supplemented with 50 ng/mL primocin (Invitrogen, ant-pm-05) for the first 4 days. The following culture was performed with the basic UCCM medium for 7–10 days. These epithelial-like urine cells were digested with 0.25 % trypsin–EDTA (GIBCO, 25200072) and seeded in a new 6 cm dish. In about 1–2 weeks, these hUCs would achieve confluence and be allowed to passage or perform reprogramming experiments.

2.2. UiEPCs generation by reprogramming hUCs

Electrical transfection with episomal vectors (pEP4EO2SET2K and pCEP4-miR-302-367) was performed on the hUCs (about 1.5 × 10^6–2.0 × 10^6) at passage1-2. The electric transfer kit was the AmaxaTM Basic Nucleo-fectorTM Kit (Lonza, VPI-1005). The treated cells (about 2.5 × 10^5) were plated on a well of 12-well plate, which is pre-coated with Matrigel (Corning, 354230). The culture lasted 3–6 days in the UCCM medium until 60 % confluence was reached. Then, the culture medium was changed to induction medium, which contained Advanced DMEM/F12 (Gibco, 12634-010), 3 μM CHIR99021 (Targetmol, T2310), 10 ng/mL bFGF (PeproTech, P09038), 10 ng/mL EGF (R&D systems, 236-EG), and 1 μM EPZ5676 (Selleck Chemicals S7062). The induction medium was refreshed every 2 days for 8–12 days when the epithelial-like cells appeared to form many clusters. Next, the culture medium was changed to UiEPCs induction medium, which contained Advanced RPMI 1640 (GIBCO), 1 × L-GlutaMAX (GIBCO, 35050-061), 1 × non-essential amino acids (NEAA; GIBCO, 11140-050), 1 × B27 (GIBCO), 1 × N2 (GIBCO), 0.1 mM β-ME(SIGAMA), 0.5 μM RG108 (TOPSCIENCE), 2 μM P8511 (TOPSCIENCE), 100 ng/mL Activin A (PeproTech), 2 μM LYZ294002 (TOPSCIENCE), 1 μM EPZ011989 (TOPSCIENCE), 100 μM NaB (TOPSCIENCE) for 8–12 days.

2.3. Differentiation of UiEPCs into U-iIOs

To induce midgut/hindgut endoderm cells, the UiEPCs were treated with 200 ng/mL Noggin (PeproTech), 10 μM SB431542 (Selleck), 500 ng/mL FGF4 (R&D Systems), 2 μM CHIR99021 (Sigma) and 1 μM SAG (R&D Systems) for 4 days in a basal medium which contains DMEM/F12 (GIBCO), 1 × L-GlutaMAX (GIBCO), 1 × B27 (GIBCO), 1 × N2 (GIBCO), 50 μg/mL Vc (Sigma), 0.4 mM MTG (Sigma). Next, to induce intestine progenitor cells, the cells were then treated with 3.5 μM CHIR99021, 20 ng/mL BMP4 (R&D Systems), and 0.5 μM RA (Sigma) in basal medium for 7–10 days. Afterward, the big and uniform cell clones were picked cut into two pieces, and cultured in two different wells with U-iIO medium, which contained 10 ng/mL FGF7 (R&D Systems), 10 ng/mL FGF10 (R&D Systems) and 3 μm CHIR99021 in basal medium. After 5–7 days, the cells in one well were used for testing the CDX2 expression. If CDX2 was stained positively, the cells in another well were resuspended and embedded in 50 μL Matrigel (Corning 354234) droplets for further validation.

2.4. Passaging of 3D U-iIOs

U-iIOs were released from Matrigel by Cell Recovery Solution (Corning, cat. no. 354253) according to the manufacturer's instructions. After release, organoids were treated with 500 μl of 0.05 % trypsin-EDTA for 2min and stopped by 10 % FBS. All solid contents were spun down at 250×*g* for 5 min. After centrifugation, organoids were pipetted gently and resuspended in fresh Matrigel droplets cultured in U-iIOs medium supplemented with growth factors 20 ng/mL HGF and 20 ng/mL OSM.

2.5. Transplantation of U-iIOs on the chick chorioallantoic membrane (CAM)

Fertilized eggs were obtained from a commercial supplier in Qingyuan City (Guangdong, China). Eggs were incubated in a humid atmosphere in an incubator at 37.5 °C. At embryo day (ED) 3.5, 2 mL of albumin was extracted from the eggs using a number 21G needle. A small window was then opened by cutting through the eggshell and sealed with a breathable membrane. On days 8–9, the aggregated U-iIOs were implanted on the CAM surface on days 15–17 and incubated for another 7 days.

2.6. Immunostaining and confocal imaging

Fixed cells or slides were permeabilized by 0.2 % Triton X-100 for 30 min and incubated in blocking buffer (PBS supplemented with 5 % FBS, 2.5 % BSA) for 1 h at room temperature (RT). Samples were washed in PBS with 0.01 % Tween 5min for 3 times. The permeabilized cells were incubated with primary antibodies overnight at 4 °C and then incubated with Alexa-Fluor secondary antibodies at RT for 1 h. At last, nuclei were stained with DAPI (Sigma, lot. D9542) for 2 min at RT. The immunofluorescence images were taken with an LSM800 confocal microscope(Carl Zeiss). The antibodies and associated information are provided (Additional file: Table S1).

2.7. Quantitative RT-PCR (qRT-PCR)

Total RNA was isolated using RNA-easy Isolation Reagent (HyClone, SH30022.01), and 2 μg RNA was reverse transcribed using a group containing: dNTP (TOYOBO, A3477L), oligo 18T (TakaRa, code D511), RT Ace (TOYOBO A3477L), RRI (TakaRa, D2313A), 5XRT Buffer (TOYOBO, A3477L). Then, qRT-PCR was carried out using an iTaq™ Universal SYBR® Green Supermix (Bio-rad #1725124) and a CFX Connect PCR machine (Bio-Rad). GAPDH was used as the housekeeping gene. Values were calculated by the delta CT method and all data were analyzed in triplicates. Two-tailed Student's t-test was used to determine the statistical significance between the control and test groups. The analysis was performed using GraphPad Prism.

2.8. Live imaging

The 3D U-iIO was mixed with Matrigel and placed on a 12-well plate so that the whole gel would be as thin as possible (<1 mm). Live cell imaging was performed with a Nikon BioStation con-focal microscope. Spherical organoids with diameters of 50–150 μm were chosen for recording. Differential interference contrast (DIC) and fluorescent images were acquired for 3–5 h at 20 min interval. After the first-round recording, the culture medium in the well was replaced with 2 mL of pre-warmed medium containing Rh123 (Sigma, SKU 83702-10 MG, 0.5 μM) or FD4 (Fluorescein isothiocyanate–dextran, Sigma, 1 μM). A normal epi-fluorescence microscope was also used to capture the phase contrast and fluorescent image of U-iIOs for 12–24 h with the same operation.

2.9. Bulk RNA-seq data analysis

The open-source software RSEM [23] and bowtie2 were used to do the alignment of paired-end sequenced reads to a transcriptome index generated from the GENCODE annotations transcriptome (hg38). The input of the downstream differential expression analysis was the calculated Transcripts Per Kilobase Million (TPM) values. We selected the top 5000 highly variable genes for principal component analysis (PCA) and correlation analysis. We used a criterion that log2(fold change) > 1 as a threshold to filter out the differentially expressed genes. Gene ontology (GO) enrichment analysis was performed using the R package clusterProfiler [24]. All statistical analyses were conducted in R(v4.1.3) and figures were plotted using the R package ggplot2 and pheatmap.

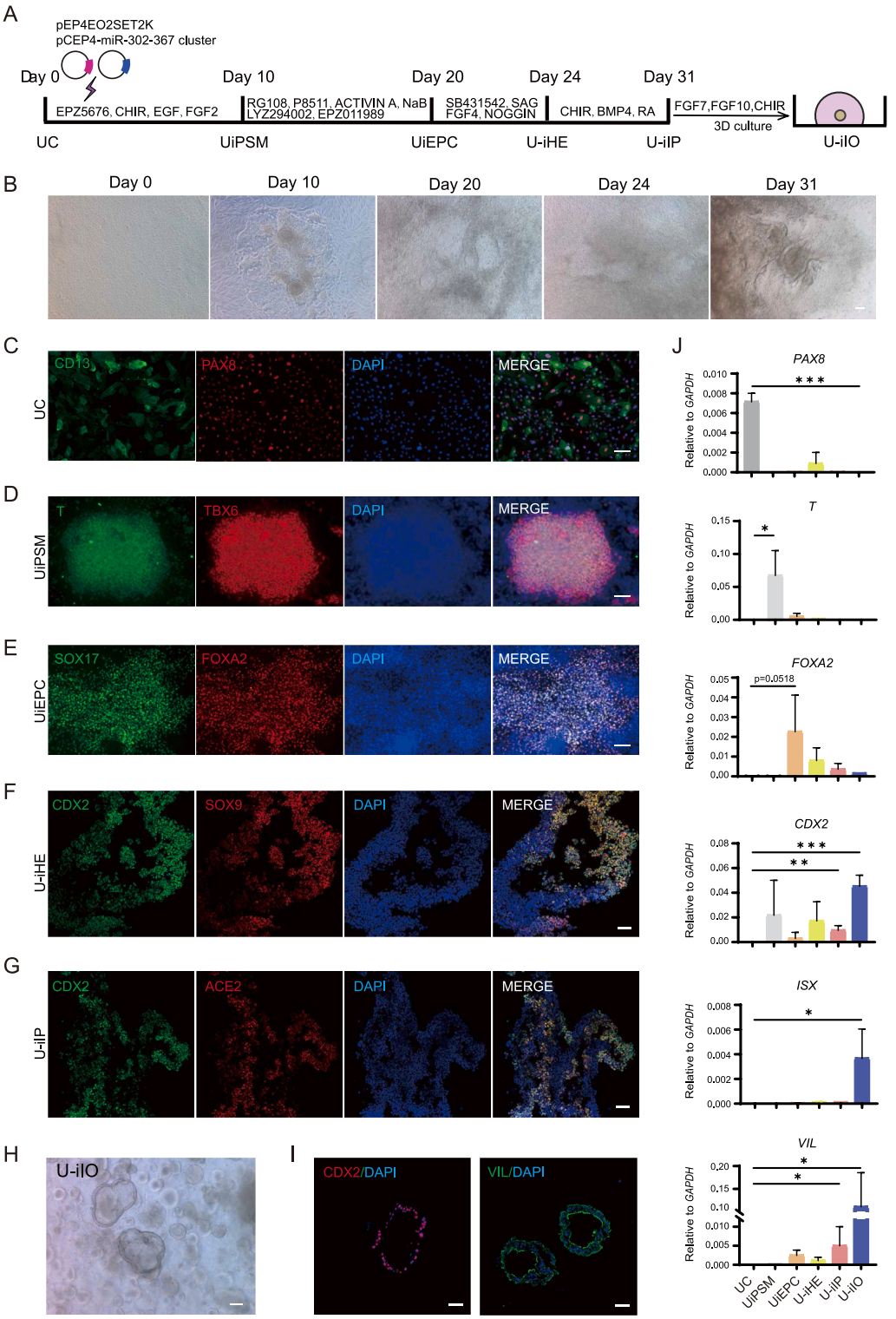

Fig. 1. Generation of intestinal organoids from hUCs. (A) Schematic illustration of UC reprogrammed into UiEPC and induced into intestinal organoids (U-iIOs). (B) Representative bright-field images taken at different stages. On day 0, hUCs are drop-shaped cells. On day 10, the polygon-shaped UiPSM cells appeared and started to form clones. On day 20, UiPSM converted to UiEPC and formed more condensed clones. On day 24, U-iHE cells formed flat clones. On day 31, U-iIP cells formed complex-shaped clones with clear boundaries. (C) Immunofluorescence images of frozen sections of UC. Green: CD13. Red: PAX8. Blue: DAPI. (D) Immunofluorescence images of frozen sections of UiPSM. Green: T. Red: TBX6. Blue: DAPI. (E) Immunofluorescence images of frozen sections of UiEPC. Green: SOX17. Red: FOXA2. Blue: DAPI. (F) Immunofluorescence images of frozen

sections of U-iHE. Green: CDX2. Red: SOX9. Blue: DAPI. (G) Immunofluorescence images of frozen sections of U-iIP. Green: CDX2. Red: ACE2. Blue: DAPI. (H) Cellular morphology diagrams of U-iIOs. (I) Immunofluorescence images of frozen sections of U-iIOs. Red: CDX2. Green: VIL. Blue: DAPI. (J) qPCR analysis for markers of UC (PAX8), primitive streak (T), endodermal cells (FOXA2), intestinal (CDX2, ISX), and intestinal villi (VIL1) during U-iIOs induction. All bars scale 50 μm. The relative expression of each transcript to GAPDH expression is presented as the mean ± SD (n = 3). *p < 0.05, **p < 0.005, ****p < 0.0001.

2.10. ScRNA-seq analysis

To compare the maturity of U-iIOs with that of the human small intestine at different developmental stages, we collected scRNA-seq data from the human small intestine at 7, 10, 11, 17, and 19 pcw (post-conception weeks) [25], and adult small intestine tissue samples [26]. We generated pseudo-bulk RNA-seq data by summing counts across all cells of each scRNA-seq sample. Counts were normalized using the voom() function of the limma R package [27] and subjected to principal component analysis (PCA).

To examine the expression of transepithelial transport-related genes in scRNA-seq data, we collected single-cell data from three different morphologic regions of the small intestine [28] (duodenum, jejunum, and ileum). We used the Python library Scanpy [29] (v1.9.6) to re-analyze the data and identify the first 2000 highly variable genes (HVG) using the function 'pp.highly_variable_genes'. HVGs were conducted for PCA and then found the neighbors for each cell with 50 principle components (PC). UMAP was used for dimensionality reduction and visualization in 2D space with the function 'tl.umap'.

2.11. Availability of data and materials

All bulk RNA-seq data from our experiments can be found on Gene ExpressionOmnibus (GEO), accession number GEO: GSE230718.

To compare the functional characteristics of U-iIOs with those from different organoid protocols and human intestinal tissues, we collected and reanalyzed data from PSC-derived organoids, as well as data from tissue biopsy samples. The published intestinal sample data used in this paper were mostly downloaded from the public database GEO: small intestine samples from GSE159751, pluripotent stem cell-derived HIOs samples from (GSE128922, GSE84666, GSE159201), human colon cancer cell line samples Caco-2 from GSE203549, HT-29 from GSE197947. Other published datasets used in this paper are scRNA-seq data of developing human early small intestine [25] (ArrayExpress: E-MTAB-9363); small intestine processed scRNA-seq datasets [28] (available at https://doi.org/10.5061/dryad.8pk0p2ns8).

3. Results

3.1. U-iIOs generation through direct reprogramming

Anatomically, the human endoderm arises from mesendoderm and gives rise to the foregut, midgut, and hindgut as development proceeds. The midgut and hindgut subsequently generate small and large intestines respectively [30]. We previously established a robust approach to generate and expand hUCs-induced presomatic mesoderm (UiPSM) [31] which expressed high levels of some mesendoderm typical genes like T, TBX6, MIXL1, and CDX2. Notably, CDX2 was also one of the critical fate determinators of intestinal epithelial cells [32]. We hypothesized that endodermal and intestinal lineage cells can be induced directly from UiPSM. To test it, we chose UiPSM as reprogramming intermediator cells and reviewed small molecules used in endodermal and intestinal progenitor cell induction protocols. The signaling activators ACTIVIN A and LYZ294002 were first added into the chemical cocktail for induction, which has been shown previously to guide and enhance endoderm progenitor cell differentiation (Fig. 1A). We also screened epigenetic inhibitors to assist overcome some barriers to cellular reprogramming. Through further optimization, we identified that one chemical cocktail containing ACTIVIN A, LYZ294002, and epigenetic inhibitors EPZ011989, NaB, RG108, and P8511 could convert UiPSM into SOX17+/FOXA2+ endoderm progenitor cells directly at day20 (Fig. 1A and B). Followed by step-wise treatment and differentiation, hUCs-induced endoderm progenitor cells (UiEPCs) were guided into hindgut fate and then intestinal epithelial cells (Fig. 1A and B). The cell fate transitions at each reprogramming stage were validated by immunofluorescence staining (CD13/PAX8 for hUCs, T/TBX6 for UiPSM, CDX2/SOX9 and CDX2/ACE2 for intestinal epithelial cells) (Fig. 1C–G). These epithelial cell clusters were picked up and embedded into Matrigel for 3D culture. The results revealed that these epithelial cells formed hollow spheroid structures (Fig. 1H), which were positive for CDX2 and VIL (Fig. 1I). Consistent with protein levels, qRT-PCR results of cell samples at different stages showed that the expression of PAX8 (specific for hUCs) decreased, while T(specific for UiPSM), FOXA2(specific for UiEPC), and CDX2/ISX/VIL (specific for intestinal epithelial cells) were upregulated at the corresponding reprogramming stage respectively (Fig. 1J). Together, these results demonstrated that intestinal organoids could be generated from human urine cells through direct reprogramming under defined mediums within one month.

3.2. Characterization of U-iIOs

To further characterize the lineage identity of U-iIOs, RNA-seq was performed for U-iIOs and hUCs. Meanwhile, we chose previously reported RNA-seq data of primary intestinal tissues from clinical biopsies as positive controls [26]. Hierarchical clustering and PCA analysis of hUC, U-iIOs and primary small intestines showed that U-iIOs and primary small intestines had similar transcriptional characteristics (Fig. S1). The average of hUCs data from three samples was selected as a reference, and U-iIOs or primary intestinal

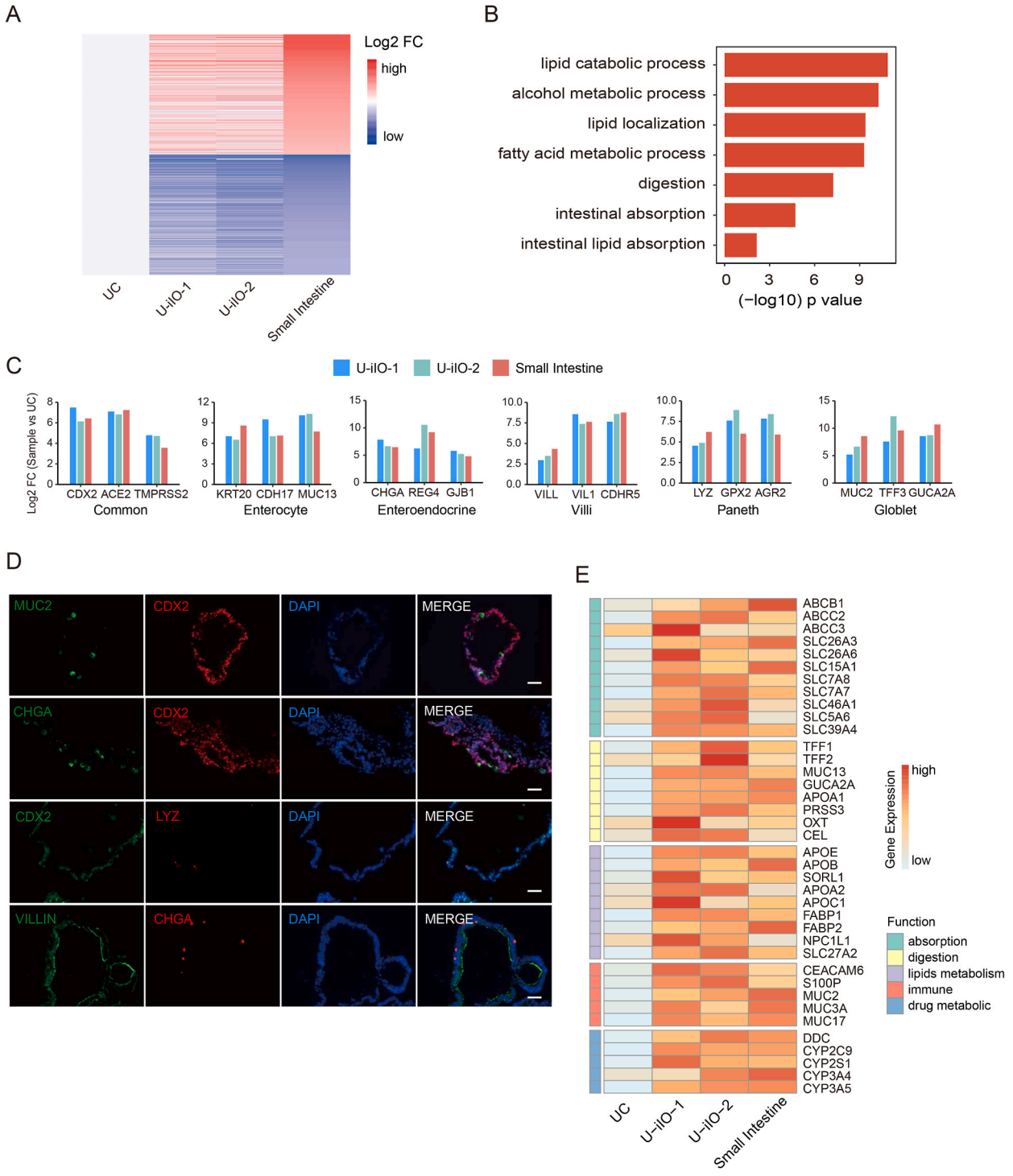

Fig. 2. Intestinal lineage identity verification. (A) Heatmap shows a similar gene regulation pattern in U-iIOs and small intestine (published small intestine tissue samples as positive control). log2(FC) was obtained by differential expression analysis with UC. (FC, fold-change). (B) Gene ontology (GO) analysis for upregulated expressed genes of U-iIOs compared to UC. (p value at the bottom). (C) Differential expression analysis showed that U-iIOs, as well as small intestine, significantly upregulated their intestinal lineage genes compared with UC. (D) Immunofluorescence images of frozen sections of U-iIOs. CDX2/MUC2, CDX2/CHGA, CDX2/LYZ, and VIL/CHGA were co-staining. Blue: DAPI. All bars scale 50 μm. (E) Gene expression analysis for intestinal function genes by RNA-seq.

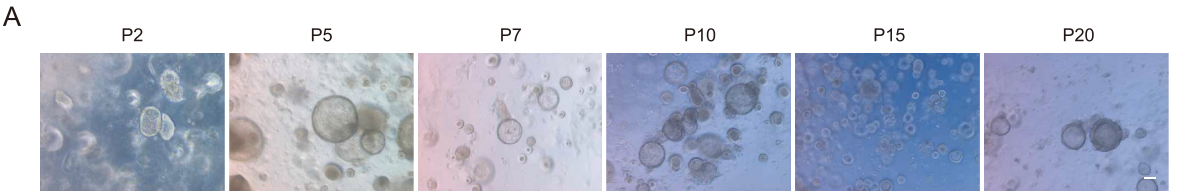

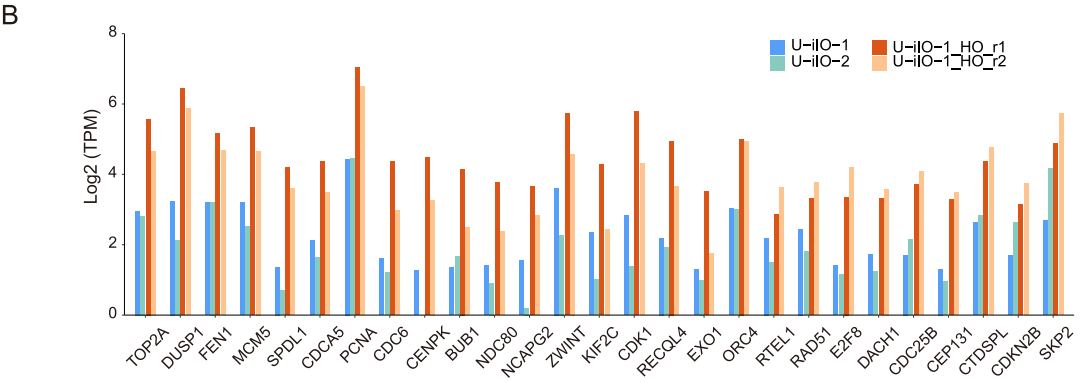

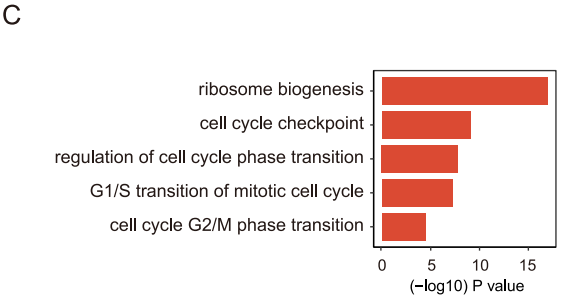

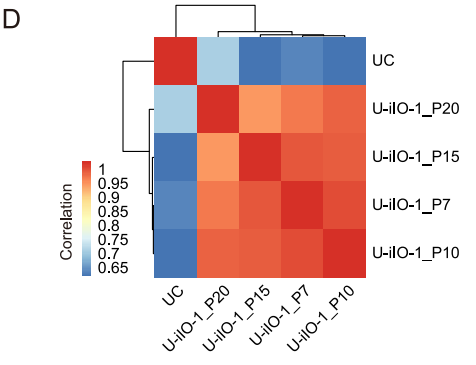

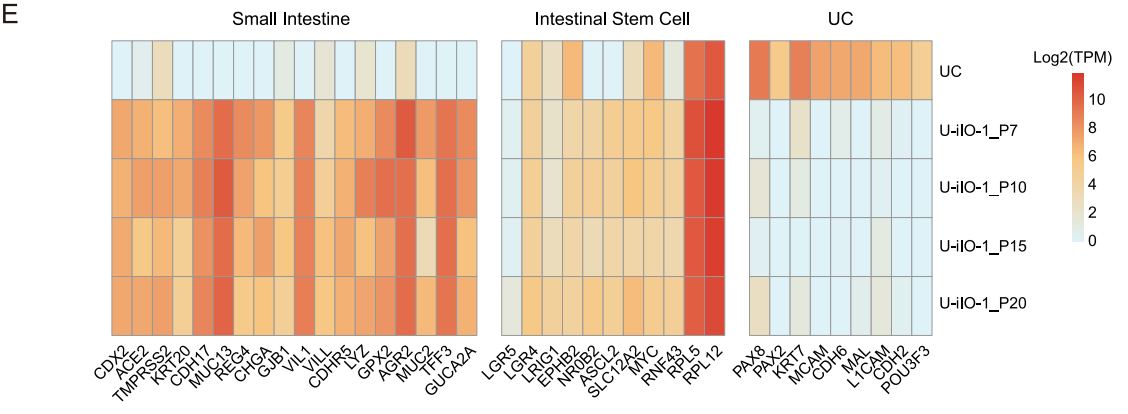

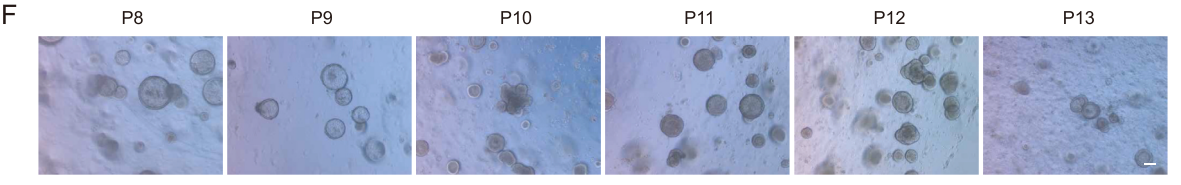

(caption on next page)

Fig. 3. U-iIOs can passage and sustain growth. (A) The cell morphology diagram showed that the organoid's morphology remained consistent during the passage. (B) The bar graph shows the difference in the expression of cell proliferation-related genes between the passaged U-iIOs samples (U-iIO-1_HO_r1 and U-iIO-1_HO_r2 which were treated with HGF and OSM. HO: HGF and OSM.) and the control sample (U-iIO-1 and U-iIO-2). (TPM, transcripts per million). (C) Gene ontology (GO) analysis for upregulated expressed genes in the passaged U-iIOs samples compared with those in the control sample. (p value at the bottom). (D) Correlation analysis shows gene expression profiles of UC and U-iIOs maintained in different passages. (E) Heatmap shows the expression of intestinal lineage genes, intestinal stem cell markers, and UC markers during the maintenance passage of U-iIOs. (F) The cell morphology diagram showed that the organoids were still able to passage after resuscitation. All bars scale 50 μm.

tissues were compared with hUCs differential gene analysis. The results showed that U-iIOs and positive control had similar gene regulation patterns (Fig. 2A). Gene ontology (GO) analysis showed that the overlapping up-regulated genes in U-iIOs and positive control were mainly enriched for physiological processes related to lipid metabolism, intestinal absorption and digestion (Fig. 2B). Based on typical marker genes of small intestines, we found that U-iIOs highly expressed KRT20/CDH17MUC13 for enterocytes, CHGA/REG4/GLB1 for enteroendocrine cell, LYZ/GPX2/AGR2 for paneth, VILL/VIL1/CDHR5 of villus, and MUC2/TFF3/GUCA2A for goblet cells, which resembled small intestine *in vivo* (Fig. 2C). Consistent with transcription levels, CDX2/MUC2, CDX2/CHGA, CDX2/LYZ and VIL/CHGA were co-staining positively further confirming the existence of intestinal lineage differentiated cells in U-iIOs (Fig. 2D).

Considering the usage of hUCs as reprogramming initiator cells and the direct reprogramming approach, we explored whether U-iIOs had small intestine specific molecular features. Not surprisingly, gene expression data showed that U-iIOs highly expressed multiple transporter genes such as the SLC family [33] and ABC family [34], two major transporter families related to absorption function, including SLC26A6 and SLC26A3 (sodium absorption and transport), SLC5A6 (intestinal vitamin absorption), SLC7A8 (cationic amino acid absorption and transport), ABCB1 and ABCC2 (xenobiotics pumping and organic anion transport) (Fig. 2E). In addition, the genes related to small intestinal digestion obviously increased, such as TFF1 and TFF2, which are trilobal peptide genes for repairing the small intestinal surface and OXT which regulates nutrient absorption (Fig. 2E). As for the immune response, MUC2, MUC17, S100P and CEACAM6 which are related to the occurrence of Crohn's disease remarkably unregulated (Fig. 2E). Lastly, U-iIOs were also enriched in APOE, APOB, and NPC1L1, which are responsible for lipid metabolism [35], as well as CYP3A4 and CYP3A5 genes for P450 enzymes [36] related to detoxification (Fig. 2E). These molecular features of U-iIOs were closely associated with intestinal key functions, suggesting that our U-iIOs might work as one promising model to study intestinal diseases and drug screening in a personalized fashion.

Taken together, these results demonstrated that molecular characteristics of U-iIOs resembled small intestine *in vivo* based on high expression of typical markers of multiple small intestine lineage cell types and genes representative of small intestine specific functions.

3.3. U-iIOs expand long-term in vitro

We wondered whether U-iIOs can be steadily expanded and maintained *in vitro* for a long time. We tried to passage U-iIOs through single cells or clusters and observed that U-iIOs proliferated poorly and couldn't expand further. Thus, we screened and added some growth factors to stimulate U-iIOs proliferation. Surprisingly, we found that hepatocyte growth factor (HGF) and oncostatin M (OSM) which were reported to promote hepatocyte maturation together enhanced U-iIOs proliferation and expansion (Fig. 3A and B). Indeed, consistent with daily observation, We collected passaged U-iIOs samples for RNA-seq and found that HGF and OSM treatment remarkably upregulate proliferating associated genes such as TOP2A, PCNA and CDK1 (Fig. 3B). GO analysis showed that these up-regulated genes were enriched for physiological processes related to cell cycle regulation and ribosome biogenesis (Fig. 3C). Under this optimizing culture condition, U-iIOs grew in ring-like structures and maintained stable transcription profiles for more than 20 passages *in vitro* (Fig. 3A–D). U-iIOs highly expressed some intestinal stem cell genes like ASCL2, a transcription factor that controls the maintenance of intestinal stem cells (ISCs); LGR4 [37], a homolog of LGR5 that also regulates the characterization of ISCs; and LRIG1 [38], which regulates the activity and quiescence of adult stem cells (Fig. 3E). Furthermore, U-iIOs could be cryopreserved and thawed to survive and expand long-term (Fig. 3F). These results suggested personalized intestinal organoid banks could be established under defined medium through direct reprogramming in the future.

3.4. U-iIOs differ from P-iIOs

To explore the differences between U-iIOs and the widely reported P-iIOs [6–8], we downloaded these reported RNA-sequencing data of P-iIOs and made detailed comparisons. The PCA analysis showed that passaged U-iIOs samples were tightly clustered, while other samples showed significant transcription differences (Fig. 4A). Next, differential gene analysis was performed (U-iIOs passage sample vs hUCs, P-iIOs vs iPSCs), and Venn diagram was drawn for up-regulated gene set. There were 119 overlapping up-regulated genes, and 801, 205, 1644, and 787 genes were specifically highly expressed in U-iIO-P, P-iIOs-1, P-iIOs-2, and P-iIOs-3, respectively (Fig. 4B). Gene ontology was performed on the identified differentially expressed genes. Terms indicative of the basic small intestine physiological processes (digestion, small intestine absorption, immunity, lipid transport, etc.) were identified in the overlapping up-regulated genes, indicating that all these samples shared basic characteristics of the small intestine (Fig. 4C). As for specific highly expressed genes, U-iIOs were specifically enriched for the physiological processes of drug metabolism and transmembrane transport while three P-iIOs focused on the response to the drug, embryonic organogenesis, and ATP synthesis respectively (Fig. 4C). Besides, we also compared the DEG of iPSC and U-iIO and obtained similar results (Fig. S2). Meanwhile, the expression level of specific intestinal

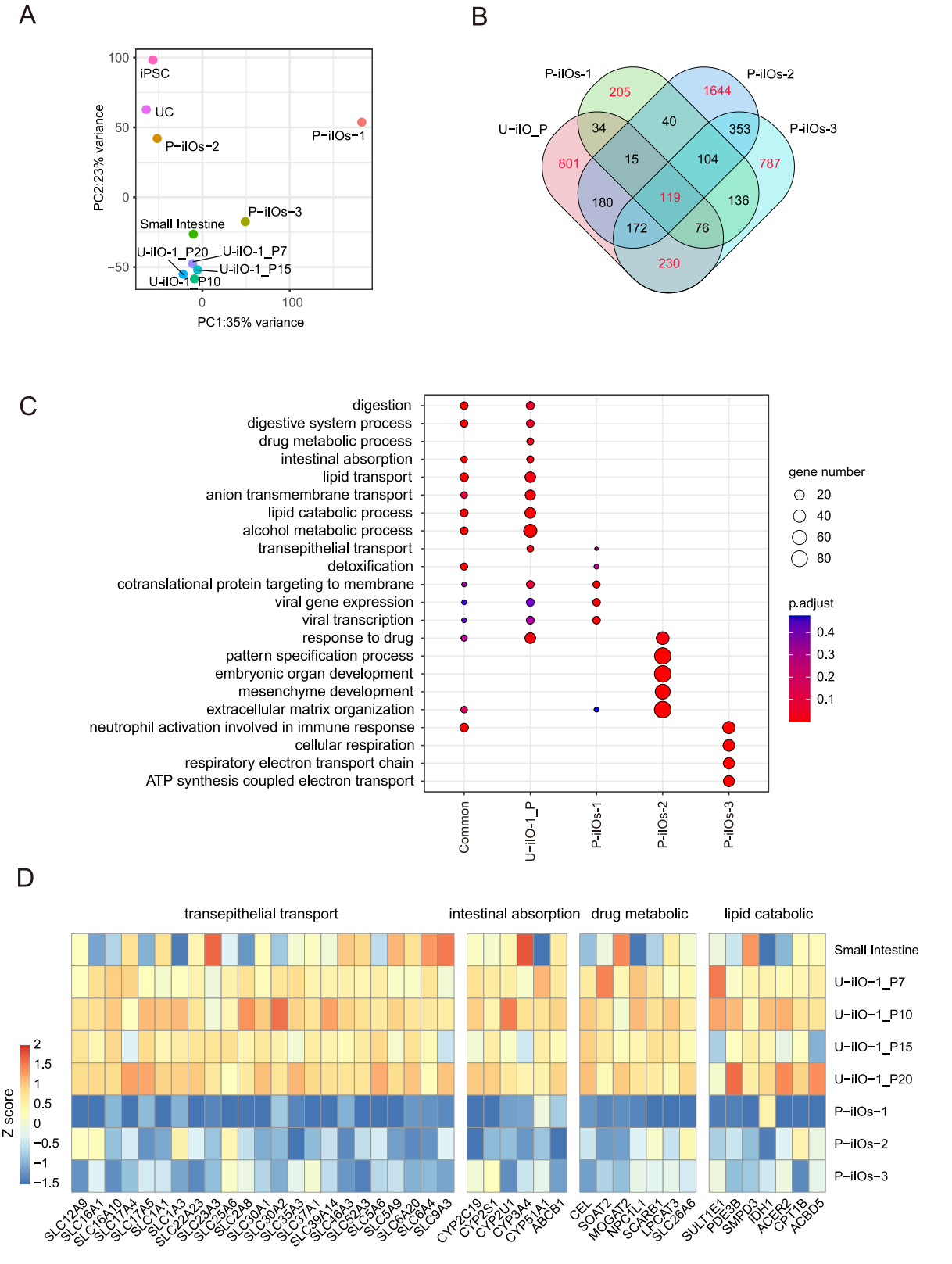

(caption on next page)

Fig. 4. Transcriptome comparison of U-iIOs and P-iIOs. (A) Principal-component analysis (PCA) of UC, iPSC, Small Intestine, passaged U-iIOs samples and human pluripotent stem cells derived intestinal organoids (P-iIOs). (B) Venn diagram shows the intersection of up-regulated genes (passaged U-iIOs samples compared with UC, P-iIOs compared with iPSC). (C) Significantly enriched GO terms were identified from the list of specifically up-regulated genes as well as overlapping up-regulated genes in the Venn diagram. The color and size of the circles indicate the P. adjust and the gene number of the GO term, respectively. (D) Heatmap shows a comparison of functional representative gene expression.

functional genes in U-iIOs and P-iIOs were compared exactly, which revealed that genes relevant to intestinal transporter and absorption, and drug metabolism enriched more obviously in U-iOs than P-iIOs (Fig. 4D). These results suggested U-iIOs differed from P-iIOs and intestinal organoids obtained by different protocols have different characteristics resulting from their starting cells with different backgrounds and propensities as well as induced conditions.

3.5. Matured U-iIOs are rich in metallothionein and CYP450

Organoid maturation is vital for downstream functional applications. As U-iIOs expand long-term and possess some molecular features of ISCs, we wanted to find out whether U-iIOs could be induced to be further mature. To validate it, we tried to promote U-iIOs further maturation through the addition of fetal bovine serum (FBS) which contained abundant nutrients critical for cell differentiation to expansion medium [39]. The results of qRT-PCR showed that FBS significantly increased the expression of typical intestinal differentiated lineage markers CDX2, ISX, MUC2, LYZ, KRT20, and VIL1 (Fig. 5A). Interestingly, we performed RNA-seq for further analysis and noticed that FBS upregulated genes were involved in response to metal ions, detoxification of inorganic compounds, and lipid catabolic process (Fig. 5B). FBS obviously enhanced the expression of metallothionein family gene [40] in U-iIOs which played an important role in metal ion binding (Fig. 5C), dissociation, and enrichment during intracellular related physiological processes and contributes to drug metabolism and detoxification of the small intestine *in vivo*. We performed qRT-PCR to further confirm metallothionein family genes expression (Fig. 5D). In addition, drug metabolism and absorption associated genes like CYP450 family and transporters upregulated in FBS treated U-iIOs (Fig. 5E). However, the addition of epidermal growth factor (EGF) which was previously reported to be important for the bubbling and maturation of intestinal organoids had no effects on U-iIOs maturation (data not shown), indicating that U-iIOs maturation relied on distinct signaling pathway and owned special molecular characteristics. Thus, we directly compared matured U-iIOs with P-iIOs and intestinal immortalized cell lines like Caco-2 [41,42] which was widely used as a cellular model for the evaluation of the effects of new drugs on intestinal functions. The results revealed that metallothionein and transporter family genes were expressed more specifically and obviously in U-iIOs than P-iIOs and intestinal immortalized cell lines (Fig. 5E). Notably, the CYP450 family especially CYP3A4 and CYP3A5 upregulated more remarkably in U-iIOs than P-iIOs and intestinal immortalized cell lines (Fig. 5E). Last but not least, COVID-19 virus receptors ACE2 and TMPRSS2 were also highly expressed in U-iIOs (Fig. 5E). Collectively, these results demonstrated that FBS promoted U-iIOs further maturation and specifically upregulated metallothionein, CYP450, and transporter family genes which were critical for drug absorption and metabolism in intestines.

3.6. U-iIOs exhibited intestinal barriers

Intestinal barrier and polarity play a pivotal role in health and disease through the regulation of absorbing nutrients and limiting the transport of harmful antigens and microorganisms [43]. Transporter proteins present at the parietal membrane of the intestinal epithelium are mainly responsible for these processes [44]. The U-iIOs highly expressed a series of intestine specific transporter associated genes (Fig. 6A and B). Among these, P-glycoprotein (P-gp) encoded by the gene ABCB1 [45], one of a family of ATP-binding cassette transporter proteins, expressed remarkably and stably in U-iIOs at different passages (Fig. 6A). As illustrated in Fig. 6C, the interior of the circular ring represents the luminal side of the intestine, that is, the apical side (AP), and the space outside the circular ring is regarded as the blood side of the material exchange process, that is, the basolateral side (BL) [46,47]. The direction that P-gp-controls substance transfer is from the BL side to the AP side and is irreversible in the opposite direction. We incubated U-iIOs with 1 μM FITC- dextran for 12–24 h and observed no fluorescent dyes could enter into the lumen of U-iIOs while intense fluorescence existed outside (Fig. 6D). On the contrary, Rh123 [46], a self-fluorescent substrate specific to transporter P-gp, entered into the lumen and displayed clear fluorescence after incubation with U-iIOs for 12–24 h (Fig. 6E). The uptaking process of Rh123 by U-iIOs was recorded under a live cell workstation as well as a regular fluorescence microscope at manual intervals respectively which consistently showed that the internal fluorescence of U-iIOs started to appear from 30 min of incubation and gradually increased with time (Fig. 6E). These results demonstrate that U-iIOs exhibited intestinal barriers and P-gp worked as a functional transporter *in vitro*.

4. Discussion

In this study, to the best of our knowledge, we report the first attempt to generate human intestinal organoids through direct reprogramming of adult differentiated somatic cells. The whole reprogramming process was taken under a defined medium within one month. We characterized human urine cells (hUCs) induced intestinal organoids (U-iIOs) and identified U-iIOs containing multiple intestinal epithelial lineage cells and resembling small intestines *in vivo*. Moreover, we developed a defined medium for the long-term expansion of U-iIOs which could be further mature and exhibit intestinal barriers *in vitro*. Remarkably, unlike human pluripotent stem cells (hPSCs) induced intestinal organoids (P-iIOs) and intestinal immortalized cell lines, U-iIOs highly and specifically expressed metallothionein, CYP450 and transporter family genes which were essential for drug absorption and metabolism in intestines.

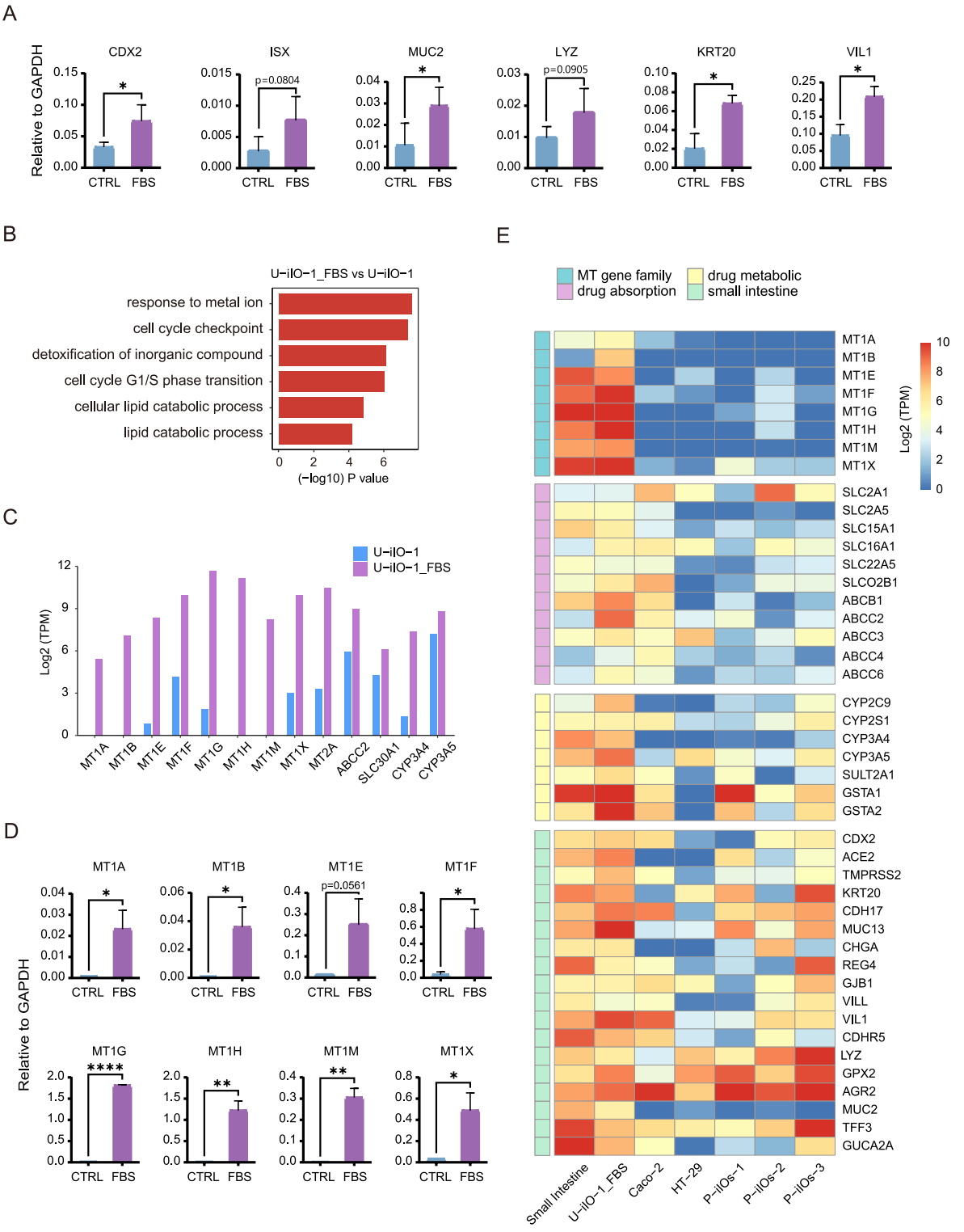

Fig. 5. The differentiated U-iIOs had functions of detoxification, drug absorption, and metabolism. (A) qPCR analysis for markers of intestinal (CDX2, ISX), goblet cells (MUC2), secretory paneth cells (LYZ), enterocyte (KRT20), and intestinal villi (VIL1) in differentiation protocols. The relative expression of each transcript to GAPDH expression is presented as the mean ± SD (n = 3). *p < 0.05, **p < 0.005, ****p < 0.0001. (B) Gene ontology (GO) analysis for upregulated expressed genes in the differentiation protocol organoids compared with those in the control medium. (p value at the bottom). (C) Bar graph shows the difference in the expression of detoxification-related genes between the differentiation protocol organoids and the control. (TPM, transcripts per million). (D) qPCR analysis for metallothionein (MT) family genes in differentiation protocols. The

relative expression of each transcript to GAPDH expression. The relative expression of each transcript to GAPDH expression is presented as the mean ± SD (n = 3). *p < 0.05, **p < 0.005, ****p < 0.0001. (E) Heatmap shows the comparison of gene expression analysis related to metallothionein (MT) family genes, intestinal lineage genes, drug absorption and metabolism.

Therefore, this study provides not only a new method to generate human intestinal organoids via direct reprogramming but also a promising *in vitro* model to investigate intestinal diseases in patient specific manners.

The intestine undertakes digestion, nutrient absorption, and waste excretion in the human body, which relies on digestive enzymes, transporters, metallothionein, and CYP450. Due to limited human intestine tissues, it is essential and significant to develop an appropriate experimental model mimicking intestinal cellular components and 3D structure *in vitro* to study human intestinal biology and diseases. In consideration of the potential tumorigenicity of hPSCs, we generated U-iIOs through direct reprogramming without going through a pluripotent state. Indeed, we transplanted U-iIOs into chick chorioallantoic membrane (Fig. S3), and subcutaneously injected them into immunodeficient mice and observed U-iIOs could not form teratoma *in vivo* (data not shown). In addition, compared with widely used reprogramming initial cells like fibroblasts and monocytes in the blood, hUCs mainly originated from kidney tubular epithelial cells and possessed some similar features to intestinal epithelial cells such as abundant transporters and mitochondria. It might be an important reason for U-iIOs own numbers of transporters. The background of different initial cell types might contribute to various features of intestinal organoids. Compared with P-iIOs, U-iIOs expressed digestion, absorption, and metabolism functional genes more obviously as well as metallothionein family genes specifically. Meanwhile, U-iIOs were enriched in COVID-19 virus receptors ACE2 and TMPRSS2. Thus, U-iIOs system would facilitate drug discovery for treating both chronic enteritis and acute infectious diseases. Long-term expansion of U-iIOs provides cellular sources for intestinal regeneration.

5. Limitations of the study

We developed one promising method for intestinal organoid generation from hUCs and confirmed intestinal organoids' identity at RNA and protein levels as well as functional validation. The differential gene comparison was performed between U-iIOs and small intestine samples and GO analysis showed that: compared to small intestine *in vivo*, U-iIOs had an upregulated function on lipids metabolism (Fig. S4B), but the immune function decreased (Fig. S4A), which might be the reason of lacking immune cells in our system. We collected some single-cell RNA-seq data from fetal intestine samples at different stages. We generated pseudo-bulk RNA-seq data by summing counts across all cells of each scRNA-seq sample and did the PCA analysis. Viewing from the PC1 axis, our U-iIOs are closer to the matured intestine samples than the fetal intestine samples (Fig. S4C). The pseudotime analysis (Fig. S4C) showed a trajectory from the fetal intestine passing the mature intestine and then to our U-iIOs, which might be a result of the up-regulation of lipid metabolism function in U-iIOs. Thus, it is important to confirm their existence and nature identities in the future by deciphering cellular components of U-iIOs by single-cell RNA-seq and comparing it directly with developing and adult intestine tissues. In addition, it remains unclear which factor in serum exactly accounts for U-iIOs maturation, which also needs to be further explored.

As for hUCs, although they were collected and isolated in a convenient and non-invasive way, not all hUCs could be successfully reprogrammed into intestinal cell fates as a result of their poor proliferation capacity. Furthermore, we can not exclude the possibility that some transporter genes enriched in hUCs are residually expressed in the intestinal organoids. Nevertheless, our study provides a novel platform to produce personalized intestinal organoids for precision medicine in the future.

Funding

This research was supported by grants from the National Key R&D Program of China (2020YFA0112400, GZNL2023A02005); the National Natural Science Foundation of China (92068201, 21907095); Key Laboratory of Guangdong Higher Education Institutes (2021KSYS009); Guangzhou Key Laboratory of Biological Targeting Diagnosis and Therapy (202201020379); Guangzhou Core Medical Disciplines Project (2021–2023) Science and Technology Planning Project of Guangzhou Province, China (2023A04J0870).

Ethics statement

The authors declare that we did not use any artificial intelligence (AI) or AI-assisted technologies in the writing process. All urine donors were provided informed consent to participate in the study.

Data availability statement

The accession number for the bulk RNA-seq data reported in this study is NCBI GEO: GSE230718.

CRediT authorship contribution statement

Ruifang Zhang: Writing – original draft, Visualization, Software, Methodology, Investigation, Formal analysis, Data curation. **Yating Chen:** Writing – original draft, Visualization, Methodology, Investigation, Formal analysis, Data curation. **Ziyu Feng:** Data curation. **Baomei Cai:** Data curation. **Yiyi Cheng:** Investigation. **Yunjing Du:** Investigation. **Sihua Ou:** Data curation. **Huan Chen:** Data curation. **Mengjie Pan:** Data curation. **He Liu:** Funding acquisition. **Duanqing Pei:** Validation, Supervision, Funding acquisition.

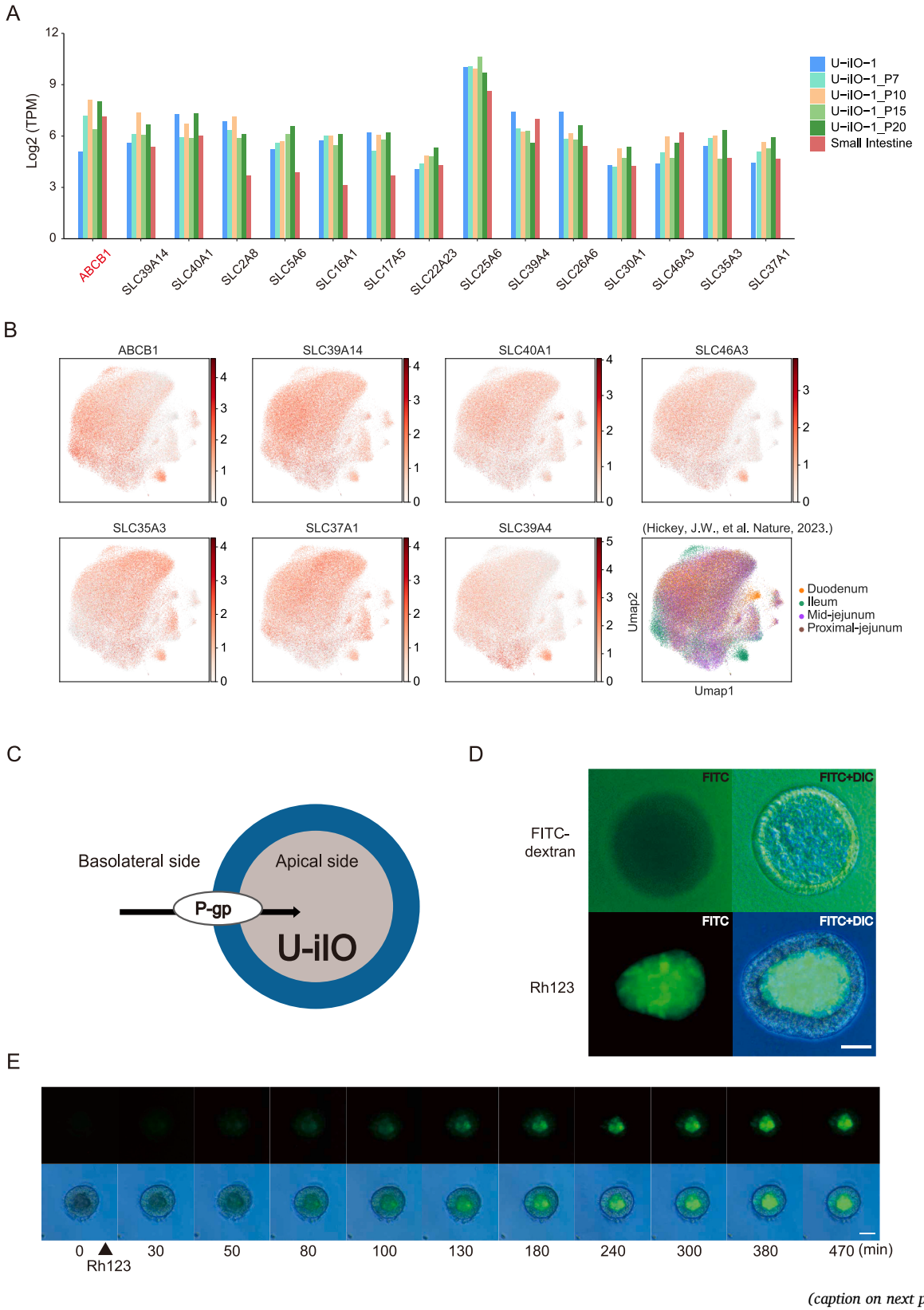

(caption on next page)

Fig. 6. Transport protein in U-iIOs had the functions of intestinal epithelial transporter. (A) The Bar graph shows the expression of transepithelial transport-related genes between the U-iIOs and the maintenance passage of U-iIOs as well as published small intestine samples. (TPM, transcripts per million). (B) Umap projection of transepithelial transport-related genes in three different morphologic regions of the small intestine: duodenum, jejunum, and ileum (data from Ref. [28]). (C) The pattern of annular intestinal organoid transporters. (D) FITC-dextran was not a substrate of any transporter and will not be transported into the apical side by the transporter. Rh123 will be transported into the internal organoid by the P-gp transporter. (E) Rh123 was gradually transported into the internal cavity of U-iIOs through P-gp transporters. All bars scale 50 μm.

Shangtao Cao: Writing – review & editing, Validation, Supervision, Resources, Project administration, Methodology, Conceptualization.

Declaration of competing interest

The authors declare that they have no known competing financial interests or personal relationships that could have appeared to influence the work reported in this paper.

Acknowledgments

We thank a lot for the human urine cell donors and are grateful for the support from the Guangzhou Branch of the Supercomputing Center of the Chinese Academy of Sciences and the Cloud Computing Center of the Chinese Academy of Sciences. We wish to thank all members of CCLA for their support.

Appendix A. Supplementary data

Supplementary data to this article can be found online at https://doi.org/10.1016/j.heliyon.2024.e33736.

References

[1] M. Gieryńska, et al., Integrity of the intestinal barrier: the involvement of epithelial cells and microbiota—a mutual relationship, Animals 12 (2) (2022) 145.
[2] A. Fatehullah, S.H. Tan, N. Barker, Organoids as an in vitro model of human development and disease, Nat. Cell Biol. 18 (3) (2016) 246–254.
[3] J. Kim, B.-K. Koo, J.A. Knoblich, Human organoids: model systems for human biology and medicine, Nat. Rev. Mol. Cell Biol. 21 (10) (2020) 571–584.
[4] N. Barker, et al., Identification of stem cells in small intestine and colon by marker gene Lgr5, Nature 449 (7165) (2007) 1003–1007.
[5] T. Sato, et al., Single Lgr5 stem cells build crypt-villus structures in vitro without a mesenchymal niche, Nature 459 (7244) (2009) 262–265.
[6] M.J. Workman, et al., Engineered human pluripotent-stem-cell-derived intestinal tissues with a functional enteric nervous system, Nat. Med. 23 (1) (2017) 49–59.
[7] A. Mithal, et al., Generation of mesenchyme free intestinal organoids from human induced pluripotent stem cells, Nat. Commun. 11 (1) (2020) 215.
[8] A. Mithal, et al., Human pluripotent stem cell-derived intestinal organoids model SARS-CoV-2 infection revealing a common epithelial inflammatory response, Stem Cell Rep. 16 (4) (2021) 940–953.
[9] S.A. Przyborski, Differentiation of human embryonic stem cells after transplantation in immune-deficient mice, Stem Cell. 23 (9) (2005) 1242–1250.
[10] A. Brederlau, et al., Transplantation of human embryonic stem cell-derived cells to a rat model of Parkinson's disease: effect of in vitro differentiation on graft survival and teratoma formation, Stem Cell. 24 (6) (2006) 1433–1440.
[11] U. Ben-David, N. Benvenisty, The tumorigenicity of human embryonic and induced pluripotent stem cells, Nat. Rev. Cancer 11 (4) (2011) 268–277.
[12] R. Dressel, Effects of histocompatibility and host immune responses on the tumorigenicity of pluripotent stem cells, in: Seminars in Immunopathology, Springer, 2011.
[13] O. Gordeeva, S. Khaydukov, Tumorigenic and differentiation potentials of embryonic stem cells depend on TGFβ family signaling: lessons from teratocarcinoma cells stimulated to differentiate with retinoic acid, Stem Cell. Int. (2017) 2017.
[14] H. Wang, et al., Direct cell reprogramming: approaches, mechanisms and progress, Nat. Rev. Mol. Cell Biol. 22 (6) (2021) 410–424.
[15] K.L. Ring, et al., Direct reprogramming of mouse and human fibroblasts into multipotent neural stem cells with a single factor, Cell Stem Cell 11 (1) (2012) 100–109.
[16] S. Zhu, et al., Mouse liver repopulation with hepatocytes generated from human fibroblasts, Nature 508 (7494) (2014) 93–97.
[17] N. Cao, et al., Conversion of human fibroblasts into functional cardiomyocytes by small molecules, Science 352 (6290) (2016) 1216–1220.
[18] T. Zhou, et al., Generation of human induced pluripotent stem cells from urine samples, Nat. Protoc. 7 (12) (2012) 2080–2089.
[19] Y. Xue, et al., Generating a non-integrating human induced pluripotent stem cell bank from urine-derived cells, PLoS One 8 (8) (2013) e70573.
[20] L. Wang, et al., Generation of integration-free neural progenitor cells from cells in human urine, Nat. Methods 10 (1) (2013) 84–89.
[21] Y. Yuan, et al., Generation of mitochondria-rich kidney organoids from expandable intermediate mesoderm progenitors reprogrammed from human urine cells under defined medium, Cell Biosci. 12 (1) (2022) 174.
[22] X.Y. Zhang, et al., MYOCD is required for cardiomyocyte-like cells induction from human urine cells and fibroblasts through remodeling chromatin, Stem Cell Reviews and Reports 18 (7) (2022) 2414–2430.
[23] B. Li, C.N. Dewey, RSEM: accurate transcript quantification from RNA-Seq data with or without a reference genome, BMC Bioinf. 12 (2011).
[24] G.C. Yu, et al., clusterProfiler: an R Package for comparing biological themes among gene clusters, Omics-a Journal of Integrative Biology 16 (5) (2012) 284–287.
[25] E.M. Holloway, et al., Differentiation of human intestinal organoids with endogenous vascular endothelial cells, Dev. Cell 54 (4) (2020) 516–528, e7.
[26] K.M. Alula, et al., Targeting mitochondrial damage as a therapeutic for ileal Crohn's disease, Cells 10 (6) (2021) 1349.
[27] C.W. Law, et al., voom: precision weights unlock linear model analysis tools for RNA-seq read counts, Genome Biol. 15 (2014) 1–17.
[28] J.W. Hickey, et al., Organization of the human intestine at single-cell resolution, Nature 619 (7970) (2023) 572–584.
[29] F.A. Wolf, P. Angerer, F.J. Theis, SCANPY: large-scale single-cell gene expression data analysis, Genome Biol. 19 (2018) 1–5.
[30] J.R. Spence, R. Lauf, N.F. Shroyer, Vertebrate intestinal endoderm development, Dev. Dynam. 240 (3) (2011) 501–520.
[31] Y. Qin, et al., Regeneration of the human segmentation clock in somitoids in vitro, EMBO J. 41 (23) (2022) e110928.
[32] S. Grainger, J.G. Savory, D. Lohnes, Cdx2 regulates patterning of the intestinal epithelium, Dev. Biol. 339 (1) (2010) 155–165.

[33] P.R. Kiela, F.K. Ghishan, Physiology of intestinal absorption and secretion, Best Pract. Res. Clin. Gastroenterol. 30 (2) (2016) 145–159.
[34] A.G. Roberts, The structure and mechanism of drug transporters, Methods Mol. Biol. 2342 (2021) 193–234.
[35] M.P. Marrades, et al., A dysregulation in CES1, APOE and other lipid metabolism-related genes is associated to cardiovascular risk factors linked to obesity, Obes. Facts 3 (5) (2010) 312–318.
[36] K.E. Thummel, Gut instincts: CYP3A4 and intestinal drug metabolism, J. Clin. Invest. 117 (11) (2007) 3173–3176.
[37] R.C. Mustata, et al., Lgr4 is required for Paneth cell differentiation and maintenance of intestinal stem cells ex vivo, EMBO Rep. 12 (6) (2011) 558–564.
[38] Y. Ji, et al., LRIG1, a regulator of stem cell quiescence and a pleiotropic feedback tumor suppressor, Semin. Cancer Biol. 82 (2022) 120–133.
[39] J. Van der Valk, et al., Fetal bovine serum (FBS): past–present–future, ALTEX 35 (1) (2018) 1–20.
[40] M. Si, J. Lang, The roles of metallothioneins in carcinogenesis, J. Hematol. Oncol. 11 (1) (2018) 107.
[41] H. Sun, et al., The Caco-2 cell monolayer: usefulness and limitations, Expet Opin. Drug Metabol. Toxicol. 4 (4) (2008) 395–411.
[42] V. Hiebl, et al., Caco-2 cells for measuring intestinal cholesterol transport - possibilities and limitations, Biol. Proced. Online 22 (2020) 7.
[43] E. Salvo Romero, et al., The intestinal barrier function and its involvement in digestive disease, Rev. Esp. Enferm. Dig. 107 (11) (2015) 686–696.
[44] P.R. Kiela, F.K. Ghishan, Physiology of intestinal absorption and secretion, Best Pract. Res. Clin. Gastroenterol. 30 (2) (2016) 145–159.
[45] S.K. Bagal, P.J. Bungay, Minimizing drug exposure in the CNS while maintaining good oral absorption, ACS Med. Chem. Lett. 3 (12) (2012) 948–950.
[46] T. Mizutani, et al., Real-time analysis of P-glycoprotein-mediated drug transport across primary intestinal epithelium three-dimensionally cultured in vitro, Biochem. Biophys. Res. Commun. 419 (2) (2012) 238–243.
[47] D. Onozato, et al., Generation of intestinal organoids suitable for pharmacokinetic studies from human induced pluripotent stem cells, Drug Metab. Dispos. 46 (11) (2018) 1572–1580.